

INITIAL STUDY OF A BLURRY INJECTOR FOR BIOFUEL

Claudia Gonçalves de Azevedo¹, Fernando de Souza Costa² and Heraldo da Silva Couto³

^{1,2}National Institute for Space Research, Associated Laboratory of combustion and Propulsion, Rodovia Presidente Dutra, km 40, Cachoeira Paulista, SP, 12630-000

³Vale Energy Solution, Rodovia Presidente Dutra, km 137,8, Eugênio de Melo, São José dos Campos, SP, 12247-004

¹claudia@lcp.inpe.br, ²fernando@lcp.inpe.br and ³and @ heraldo.couto@vsesa.com.br

Abstract: *The increasing costs of fossil fuels, environmental concerns and stringent regulations on fuel emissions have caused a significant interest on biofuels, especially ethanol and biodiesel. The combustion of liquid fuels in diesel engines, turbines, rocket engines and industrial furnaces depends on the effective atomization to increase the surface area of the fuel and thus to achieve high rates of mixing and evaporation. Blurry injectors can produce a spray of small droplets of similar sizes, provide excellent vaporization and mixing of fuel with air, low emissions of NO_x and CO, and high efficiency. This work describes the initial characterization of a blurry injector for biofuels and proposes a predictive mathematical model for the relationship between the upstream liquid properties and the operating conditions with the droplet size. Droplet size distribution and average diameters are measured by a laser system using a diffraction technique.*

Keywords: *Blurry injector, Liquid biofuels, Laser diffraction technique, Droplet size, Test bench*

1 Introduction

The continuous increase of oil prices and growing environmental concerns has raised interest in biofuels, especially ethanol and biodiesel. In addition, environmental legislation has become increasingly rigorous, setting rigid boundaries for the pollutants emissions of engines, turbines, furnaces, boilers and industrial combustion processes. Therefore, it is of interest to the country and companies to investigate the use of biofuels in industrial applications, aiming to reduce costs, increase operating efficiency and reduce pollutants emissions.

In general, before burning, liquid fuels are atomized through nozzles to form droplets, aiming to increase the contact area between the fuel and oxidizer and, therefore, to increase the rates of mixing and fuel evaporation. The reduction of droplet size leads to higher heat release rates per unit volume, facilitates the ignition of the mixture, extends the burning range and reduces the emissions of pollutants (Couto, 2007).

Many processes in the industry, in technological processes and medicine depend on the production of sprays with droplets of micrometric size. The atomization process occurs when a liquid jet, liquid sheet or a liquid film is disintegrated by the kinetic energy of the liquid itself, by exposure to a stream of air or gas of high speed, or as a result of external mechanical energy applied through rotating devices or vibrating (Lacava *et al.*, 2009). Due to the random nature of the atomization process, the resulting spray is usually characterized by a large spectrum of droplet size.

Based on a flow-focusing injector, Gañan-Calvo, 1998, developed the blurry type injector which presents several advantages over other injectors, such as formation of a uniform spray, better atomization, high atomization efficiency, robustness, excellent fuel vaporization and mixture with air, and potential for application in compact combustion systems which can be used as portable power sources. Panchasara *et al.* (2009) compared experimentally a blurry injector with a commercial air-blast injector, using kerosene and diesel burning in air at ambient pressure, and verified that the flow blurring injector produced 3 to 5 times lower NO_x and CO emissions as compared to the airblast injector. Sadasivuni and Agrawal (2009) used the blurry injector in a compact combustion system with a counter flow heat exchanger. The volumetric energy density of the system was substantially higher than that of the concepts developed previously. The combustion system produced clean, compact, quiet, distributed, attached flat flame. No soot or coking problems were experienced during or after combustor operation on kerosene fuel.

Therefore, this work aims to present the initial characterization of a blurry injector for biofuels and proposes a predictive mathematical model for the relationship between the upstream liquid properties and the operating conditions with the droplet size. This injector will be later used in a flameless compact combustor. Flameless combustion is a homogeneous low temperature burning process leading to strongly reduced pollutant emissions and higher efficiency compared to traditional combustion processes (Wüning *et al.*, 1997).

2 Operational principle of a blurry injector

There are numerous ways of finely breaking up a liquid into droplets. The blurry injector uses a second fluid, normally a gas, to provide the energy necessary to finely divide and disperse the liquid into smaller fragments or particles.

The blurry injector yields a simple, reproducible, and robust flow pattern which gives rise to a gas-liquid interaction with a high efficiency. The flow geometry surpasses the efficiency of “pre-filming air-blast atomizers,” a highly efficient albeit complex and costly technological variety. This achievement is due to the unexpected emergence of a back-flow pattern leading to small-scale perturbations (Gañan-Calvo, 2005).

The flow-blurring injector consists of a nozzle for liquid injection and an orifice plate located downstream of the nozzle. Figure 1 shows a scheme of the blurry injector.

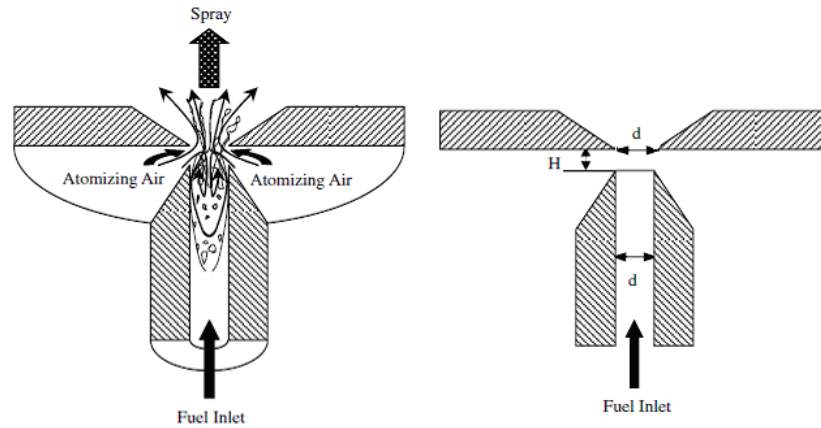


Figure 1. Schematic the Flow-Blurring Injector: flow structure and geometric details.

Reference Source: Adaptation, Panchasara, D. E., *et al.*, 2009.

The liquid to be atomized exits from a feed tube whose inner diameter is equal to the exit orifice diameter D , as seen in Fig. 1. The outlet of the feed tube has the same diameter D as the exit orifice; both sections face each other, at an offset distance H . The end of the tube is sharp cut perpendicularly to its axis. Thus, the gap between the tube end and the exit orifice gives rise to a lateral cylindrical passageway, LCP. It is worth noting that the LCP surface equals the exit orifice area when $c = H/D = 0.25$. Consequently, when both a liquid mass flow rate \dot{m}_l is forced through the tube and a gas mass flow rate \dot{m}_g is forced through the LCP, a spray combining both phases is formed and leaves the device through the orifice exit.

The bifurcation separating the back-flow regime from a conventional flow-focusing pattern is triggered by a single fundamental geometrical parameter $c = H/D$. When c is decreased to about 0.25, a radical modification in the flow configuration is observed. There is the return of the gas flow into the feeding tube of the liquid, creating a recirculation flow within the tube, resulting in an intense mixture between the phases and thus creating an almost uniform spray of small droplets. When $c > 0.25$ the liquid flow follows a “flow focusing” pattern, with the formation of a liquid microjet (Gañan-Calvo, 2005).

3 Blurry injector

A blurry injector with $D = 1$ mm was designed and built. The offset distance, H , is controlled by the action of a screw nut and can be varied from 0.15 mm to 0.30 mm. Figure 2 shows a scheme and photo of a blurry injector.

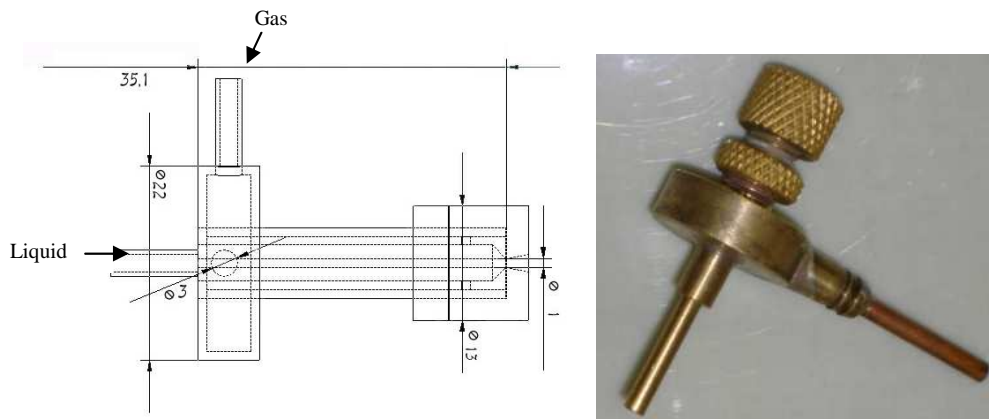


Figure 2. Schematic representation and photo of the Blurry injector.

In order to minimize gas friction losses between the tube walls and the exit orifice walls when the ratio H/D is small, the tube end was sharpened with an angle of 60° .

4 Dimensional analysis

Dimensional analysis is a classical approach from the field of fluid mechanics. In fluid mechanics, the governing equations of fluid flow are often quite complex to solve (e.g. Navier stokes equations), and instead, experiments are often used to investigate the flow phenomena. In this context, dimensional analysis is used to reduce the number of independent parameters considered and the number of tests needed to fully characterize a particular problem. The Buckingham Pi theorem states that an equation describing a phenomenon and involving N independent parameters and P independent dimensions can be reduced to a simpler equation involving N-P dimensionless numbers built on the N parameter.

The parameters involved in the breakdown and formation of liquid droplets are eminently fluid dynamics and therefore the physical properties of the liquid, operating conditions and geometry of the injector are interrelated. The correlation of the variables obtained only from experimentation is a laborious process since it requires an extensive collection of results, formation of a data base and its reduction to obtain the relations.

The dimensionless equating of sprays demand the knowledge of the physical parameter involved in the phenomenon, noting that this study focused on the correlations for the diameter of the droplets.

For analysis of the variables is initially necessary to relate the variables involved in the process of atomization in the injector. At this stage, based on the available literature on atomization, can then write to the droplet diameter d :

$$d = f(\rho_g, \rho_l, v_g, v_l, \dot{m}_g, \dot{m}_l, \sigma_l, \mu_l, D, P) \quad (1)$$

Variables involved:

Of the injector:

- D : exit orifice diameter;

Of the liquid to be atomized:

- ρ_l : Density of liquid;
- v_l : Velocity of liquid;
- \dot{m}_l : mass flow rate of liquid;
- σ_l : Surface tension;
- μ_l : Viscosity of liquid.

Of the fluid of atomization (gas):

- ρ_g : Density of gas;
- v_g : Velocity of gas;
- \dot{m}_g : mass flow rate of gas;

Then, the droplet diameter depends of the variables: $d, \rho_g, \rho_l, v_g, v_l, \dot{m}_g, \dot{m}_l, \sigma_l, \mu_l, D, P$

Thereby, have that $N = 11$ parameters, including the droplet diameter d .

Dimensions involved: M (mass), L (length), t (time), then, $P = 3$ primary dimensions.

$(N-P) = 11-3 = 8$ dimensionless groups or 8 π 's Buckingham Theorem.

Checking the parameters that are repeated, with combinations of 3 basic dimensions (M, L and T), in the simplest form: ρ_l, v_l, D .

Following, the dimensionless groups π_1 to π_8 will be presented.

4.1 First dimensionless parameter π_1 :

$$\pi_1 = \rho_l, D, v_l, d_g$$

$$M^0 L^0 T^0 = [\rho_l][D][v_l][d_g]$$

$$M^0 L^0 T^0 = [M/L^3]^a [L]^b [L/T]^c [L]$$

$$M^0 L^0 T^0 = M^a L^{-3a} L^b L^c T^{-c} L$$

$$M^0 L^0 T^0 = M^a L^{b-3a+c+1} T^{-c}$$

Solving the system of algebraic equations in a, b and c has that:

$$\pi_1 = \frac{d_g}{D} \quad (2)$$

4.2 Second dimensionless parameter π_2 :

$$\pi_2 = \rho_l, D, v_l, \rho_g$$

$$M^0 L^0 T^0 = [M/L^3]^a [L]^b [L/T]^c [M/L^3]$$

Similarly, solving the system for a, b, c has:

$$\pi_2 = \frac{\rho_g}{\rho_l} \quad (3)$$

4.3 Third dimensionless parameter π_3 :

$$\pi_3 = \rho_l, D, v_l, v_g$$

$$M^0 L^0 T^0 = [M/L^3]^a [L]^b [L/T]^c [L/T]$$

Again, solving the system for a, b and c has that:

$$\pi_3 = \frac{v_g}{v_l} \quad (4)$$

4.4 Fourth dimensionless parameter π_4 :

$$\pi_4 = \rho_l^a, D^b, v_l^c, \dot{m}_g$$

Solving the system for a, b and c has that:

$$\pi_4 = \frac{\dot{m}_g}{\rho_l v_l D^2} \quad (5)$$

4.5 Fifth dimensionless parameter π_5 :

$$\pi_5 = \rho_l^a, D^b, v_l^c, \dot{m}_l$$

Solving the system for a, b and c has that:

$$\pi_5 = \frac{\dot{m}_l}{\rho_l v_l D^2} \quad (6)$$

4.6 Sixth dimensionless parameter π_6 :

$$\pi_6 = \rho_l^a, D^b, v_l^c, \sigma_l$$

Repeating and solving the system for a, b and c has that:

$$\pi_6 = \frac{\sigma_l}{\rho_l v_l^2 D} = 1/We \quad (7)$$

4.7 Seventh dimensionless parameter π_7 :

$$\pi_7 = \rho_l^a, D^b, v_l^c, \mu_l$$

Solving the system for a, b and c has that:

$$\pi_7 = \frac{\mu_l}{\rho_l v_l D} = 1/Re \quad (8)$$

4.8 Eighth dimensionless parameter π_8 :

$$\pi_8 = \rho_l^a, D^b, v_l^c, P$$

Again, solving the system for a, b and c has that:

$$\pi_8 = \frac{P}{\rho_l v_l^2} = Eu \quad (9)$$

Rearranging the dimensionless parameters presented in order to detach the dimensionless that has the dependent variable has:

$$\pi_1 = f(\pi_2, \pi_3, \pi_4, \pi_5, \pi_6, \pi_7, \pi_8) \text{ or} \quad (10)$$

$$d_g/D = f\left(\frac{\rho_g}{\rho_l}, \frac{v_g}{v_l}, \frac{\dot{m}_g}{\rho_l v_l D^2}, \frac{\dot{m}_l}{\rho_l v_l D^2}, \frac{1}{We}, \frac{1}{Re}, Eu\right) \quad (11)$$

The function f is the function of correlation and therefore the main goal. However it is unknown a priori. It lists all the dimensionless groups that become the independent and dependent variables, all linked conditions of flow. The challenge is therefore to seek the function f through a regression model with acceptable statistical significance. Whereas the dependent variables are dimensionless groups and also based on concept of dimensional homogeneity, can be propose a regression model based on a multiplicand of factors of the type:

$$d_g/D = k \left(\frac{\rho_g}{\rho_l}\right)^a \left(\frac{v_g}{v_l}\right)^b \left(\frac{\dot{m}_g}{\rho_l v_l D^2}\right)^c \left(\frac{\dot{m}_l}{\rho_l v_l D^2}\right)^d \left(\frac{1}{We}\right)^e \left(\frac{1}{Re}\right)^f (Eu)^g \quad (12)$$

being k the constant of proportionality.

Rewriting in terms of dimensionless mass flow rates and velocities have that:

$$d_g/D = k \left(\frac{\rho_g}{\rho_l}\right)^a \left(\frac{v_g}{v_l}\right)^b (RLG)^c (We)^d (Re)^e (Eu)^f \quad (13)$$

$GLR = \dot{m}_g / \dot{m}_l$ is the gas-to-liquid mass ratio, We is the Weber number, Re is the Reynolds number and Eu is the Euler number.

The dimensionless models above lists the main parameters involved in the process of atomization. The exponents a, b, c, d, e, f and the constant of proportionality k become coefficients to determined, which are extracted statistically from the data base of experiments.

5 Spray characterization

The characterization of the blurry injector involves the determination of discharge coefficient, mean droplet sizes and spray cone angle as a function of the liquid and air tank pressures. Water was used in the initial tests.

5.1 Discharge coefficient

The discharge coefficient is used to correlate the liquid mass flow rate with the liquid pressure drop along the injector. In this case there is no air flow during the measurement.

Considering incompressible flow, adiabatic flow, no variation of gravitational potential energy, the discharge coefficient is obtained from the continuity equation (Delmeé, 1983):

$$c_d = \frac{\dot{m}_l}{A\sqrt{2\rho_l\Delta P_l}} \quad (14)$$

where $\Delta P_l = P_{l,inj} - P_{amb}$ is the drop pressure, P_{amb} is the ambient pressure and $P_{l,inj}$ is the liquid injection pressure. The liquid injection pressure is measured just before the injector and its value is about 0.1 to 0.2 bar lower than the liquid tank pressure. It is expected that the discharge coefficient does not change with liquid mass flow rate, in order to the liquid mass flow rate to vary only with $\Delta P_l^{1/2}$.

To determine the discharge coefficient, the liquid is collected in a graduated recipient during 50 s and after the liquid mass in the recipient is measured and the average mass flow rate in this period is calculated.

5.2 Mean droplet size

The laser system Spraytec® measures the size distributions of drops by laser diffraction technique, without interfering in the liquid atomized. A laser beam passes through the spray, initially parallel, and then is diffracted by the droplets. Photodiodes located on a circular plate collect the scattered light. The system uses the Mie theory for analysis of the droplet size distribution.

A commonly used representative diameter in a reactive spray is the Sauter mean diameter, SMD. It is denoted by D_{32} and is defined by:

$$D_{32} = \frac{\sum_{i=1}^n d_i^3}{\sum_{i=1}^n d_i^2} \quad (15)$$

Other representative diameters are the mass diameters D_{10} , D_{50} and D_{90} . These diameters correspond, respectively, to drop diameters that encompass 10%, 50% and 90% of total volume (or mass) of drops below the drop volume (or mass) considered. It should be noted that D_{50} is another notation for MMD.

5.3 Spray cone angle

Generally, the spray formed in the process of atomization has initially the shape of a cone. The opening angle is related to the penetration capability of the spray in the environment or combustion chamber (Lefebvre, 1989).

The spray cone angle is measured from digital photographs for each pre-defined condition. The photos are inserted into a treatment program image where two straight lines are drawn at the exit orifice tangent to the spray, allowing to measure the angle of the spray.

5.4 Experimental results

5.4.1 Discharge coefficient

Figure 4 shows the values of discharge coefficient obtained for the blurry injector with the liquid injection pressure ranging from 0.6 to 7 bar. Tests were conducted using the geometric parameter $c = H/D$ equal to 0.20 and 0.25.

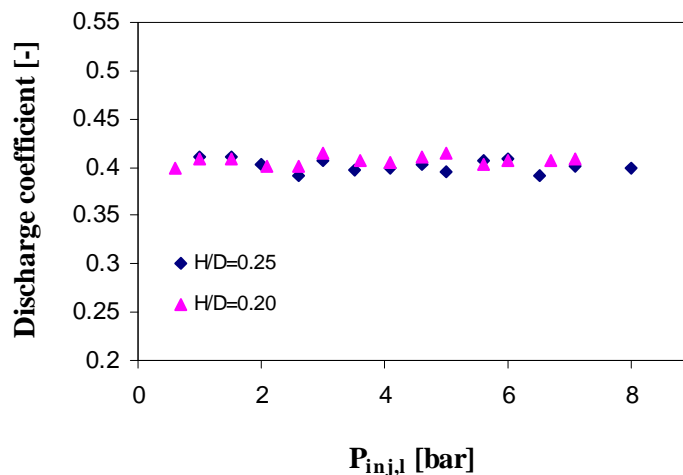


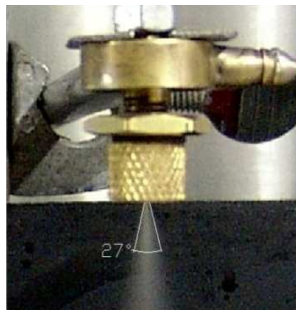
Figure 4. Discharge coefficient of the blurry injector without gas flow.

For the pressure range examined, the discharge coefficient was approximately constant, with average value 0.407 for $H/D = 0.20$ and 0.402 for $H/D = 0.25$.

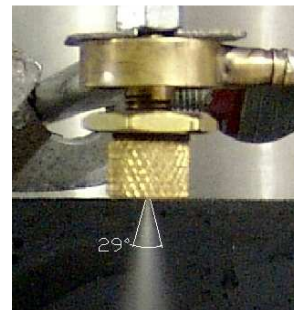
It is observed that regardless of the configuration H/D adopted the experimental values obtained for the coefficient of discharge are close. It is verified that the blurry regime also occurs for $H/D = 0.20$.

5.4.2 Spray cone angle

The spray cone angles for some operating conditions are presented in Figs. 5 and 6. In these figures $\Delta P_g = P_{g,inj} - P_{amb}$ where $P_{g,inj}$ is the injection pressure of air.

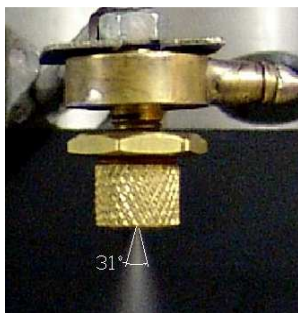


a) $\Delta P_l = 0.8$ bar and $\Delta P_g = 1$ bar.

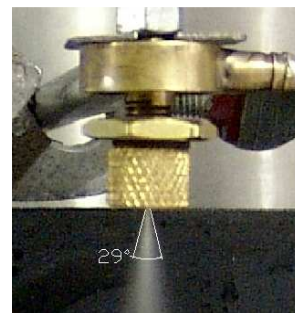


b) $\Delta P_l = 1.7$ bar and $\Delta P_g = 2$ bar.

Figure 5. Spray cone angle with $H/D = 0.20$.



a) $\Delta P_l = 0.8$ bar and $\Delta P_g = 1$ bar.



b) $\Delta P_l = 1.7$ bar and $\Delta P_g = 2$ bar.

Figure 6. Spray cone angle with $H/D=0.25$.

It is verified, in Figs. 5 and 6, an increase of spray angle for $H/D = 0.25$ compared to $H/D = 0.2$, for $\Delta P_l = 0.8$ bar and $\Delta P_g = 1$ bar. However, it is not verified a change of spray angle for $H/D = 0.25$ compared to $H/D = 0.2$, for $\Delta P_l = 1.7$ bar and $\Delta P_g = 2$ bar.

5.4.3 Mean droplet size

The experimental Sauter mean diameters and mass median diameters are presented in Figs. 7 and 8 for different injection pressures with the configurations $H/D = 0.20$ and $H/D = 0.25$.

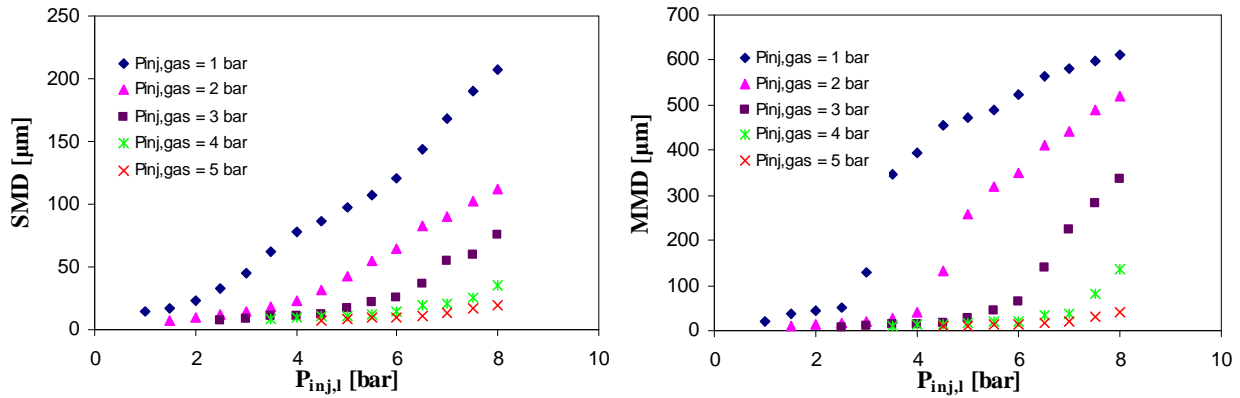


Figure 7. Experimental Sauter mean diameter (SMD) and mass median diameter (MMD) for $H/D = 0.20$.

As expected, it is observed that an increase in the injection pressure of liquid leads to an increase in SMD and MMD, and an increase in the injection pressure of air causes a decrease in SMD and MMD for both configurations. For injection pressure of air 1 and 2 bar it is observed an abrupt increase of the droplet size. For injection pressures of liquid above the injection pressure of air, air cannot flow into the liquid tube and does not mixes turbulently with the incoming liquid, there is no blurring effect, but the generation of a microjet. It is verified that SMD and MMD are smaller for $H/D = 0.20$.

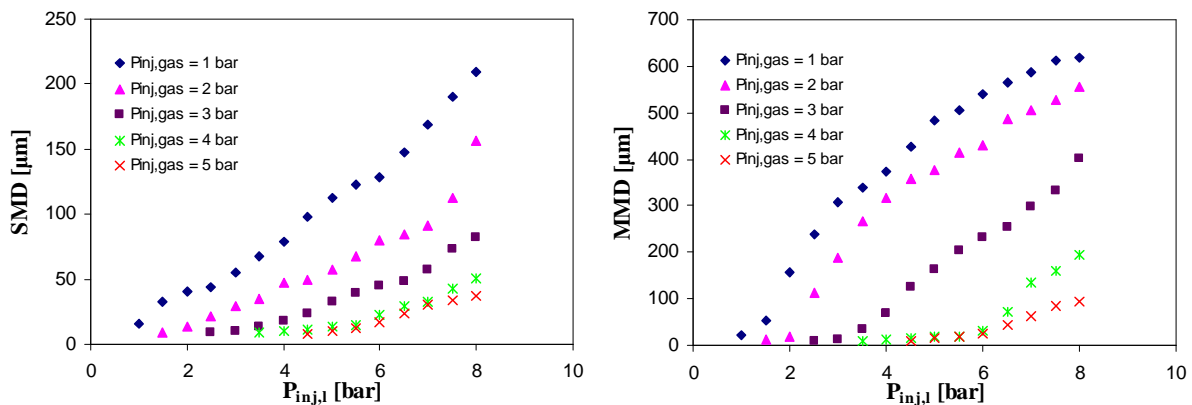


Figure 8. Experimental Sauter mean diameter (SMD) and mass median diameter (MMD) for $H/D = 0.25$.

6 Predictive Model

From the data collected in the tests was possible to verify the correlations between the parameters. For the analysis of the results was chosen using a computer program for statistical analysis as the program Statistica[®]. Using this tool allowed the various types of analysis with different methods of calculation.

Through a nonlinear regression the model prediction was finally completed. For the regression was used the "quasi-Newton" method with deviation function of the least squares.

The models of nonlinear regression with all the coefficients determined is shown in Eq. (16) for the case $H/D = 0.20$ and Eq. (17) for $H/D = 0.25$.

$$d_g/D = 0.348810 \left(\frac{\rho_g}{\rho_l} \right)^{-2.74599} \left(\frac{v_g}{v_l} \right)^{-1.72594} (RLG)^{-2.60930c} (We)^{1.427183} (Re)^{-2.61162} (Eu)^{1.888172} \tag{16}$$

$$d_g/D = 0.006409 \left(\frac{\rho_g}{\rho_l} \right)^{-1.21313} \left(\frac{v_g}{v_l} \right)^{-1.03221b} (RLG)^{-1.43625} (We)^{1.002667} (Re)^{-0.945775} (Eu)^{2.215887} \tag{17}$$

The value of regression coefficient r^2 is 0.99582 for $H/D = 0.20$ and 0.99743 for $H/D = 0.25$, classified by the authors like Barbetta (2004), as a "strong" regression.

The obtained models were subjected to a statistical evaluation for checking the quality of the regression against the phenomenon. Was observed the difference between the predicted values by the regression and those measures.

Figure 9 shows the comparison between the results obtained in measurements and those calculated by the prediction model presented in Eq (16), considering $H/D = 0.20$.

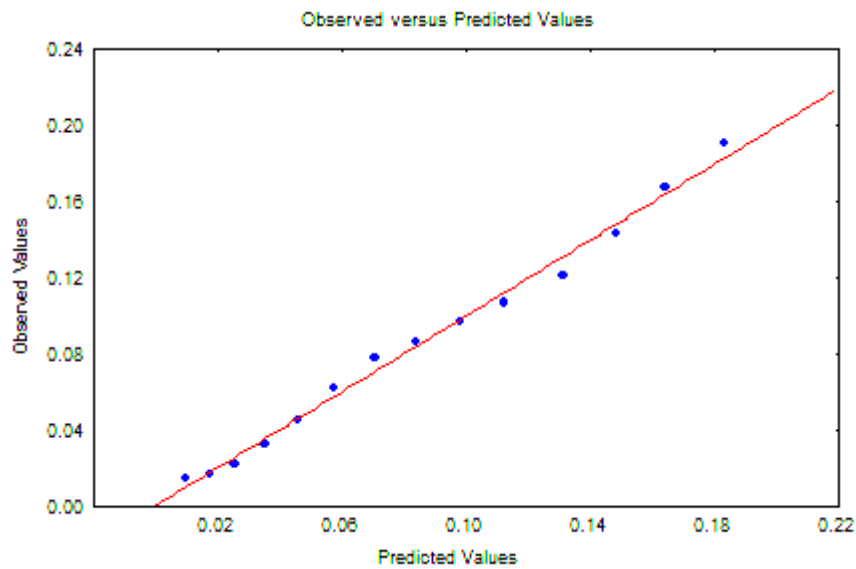


Figure 9. Correlation between predicted values by regression nonlinear and observed values for $H/D = 0.20$.

Figure 10 shows the comparison between the results obtained in measurements and those calculated by the prediction model presented in Eq (17), considering $H/D = 0.25$

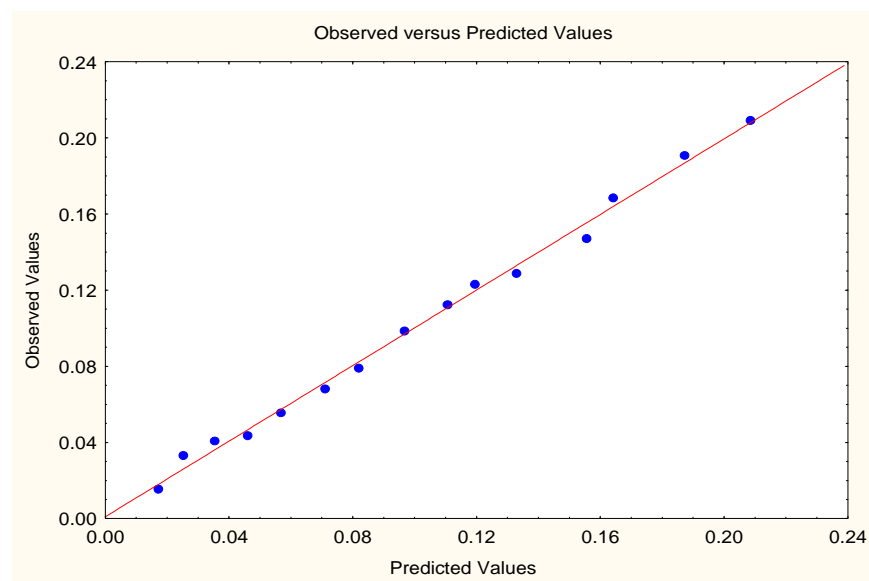


Figure 10. Correlation between predicted values by regression nonlinear and observed values for $H/D = 0.25$.

The overall results of the regression were very reasonable, due to the correlation coefficient and the residual values. It is observed an increasing trend and strong consistency between the predicted and observed values.

7 Conclusions

This paper presented the initial development of a blurry injector for burning biofuels. A bench was designed and prepared for testing the injector. Discharge coefficients, spray angles, distribution of droplet sizes and average diameters were determined experimentally.

As expected, it is observed that an increase in the injection pressure of liquid leads to an increase in SMD and MMD, and an increase in the injection pressure of air causes a decrease in SMD and MMD for both configurations. For the pressure range examined, the discharge coefficient was approximately constant, with average value 0.407 for $H/D = 0.20$ and 0.402 for $H/D = 0.25$.

The regression models extracted from the database showed statistical significant acceptable in engineering and multiple regression coefficients fully satisfactory.

Furthermore, the validation tests showed a strong coherence between values of predicted diameter when compared with measurements effective.

Acknowledgments

The authors acknowledge Vale Energy Solutions for providing a scholarship to the first author.

References

- Anderson, J. D., *Modern Compressible Flow: With Historical Perspective*, New York: McGraw-Hill Science/Engineering/Math, 3 edition, 2003.
- Barbeta, P.A *et al.*, *Estatística para Cursos de Engenharia e Informática*, São Paulo, ATLAS, 2004.
- Couto, H.S., *Atomização e Sprays*, Apostila I Escola de Combustão, Florianópolis, Santa Catarina, Brazil, 2007.
- Delmeé G. J., *Manual de Medição de Vazão*, São Paulo: Editora Edgard Blucher, 1983.
- Dodge, L.G., Change of calibration of diffraction based particle sizes in dense sprays, *Optical Engineering*, Vol. 23, No5, pp. 626-630, 1984.
- Gañán-Calvo, A. M., Generation of Steady Liquid Microthreads and Micro-Sized Monodisperse Sprays in Gas Streams, *Physical Review Letters*, Vol.80, No2, pp. 285-288, 1998.
- Gañán-Calvo, A. M., Barrero, A., A Novel Pneumatic Technique to Generate Steady Capillary Microjets, *J. Aerosol Sci.*, Vol.30, pp. 117-125, 1999.
- Gañán-Calvo, A. M., Enhanced Liquid Atomization: From Flow-Focusing to Flow-Blurring, *Applied Physics Letters* 86, 2005.
- Lacava, P. T., Alves, A., *Capítulo 3: Injeção de Combustível*, Apostila II Escola de Combustão, pp.68-111. São José dos Campos, São Paulo, Brazil, 2009.
- Lefebvre, A.H., *Atomization and Sprays*, Taylor and Francis, New York, 1989.
- Panchasara, H. V., Sequera, D. E., Schreiber, W. C., Agrawal, A. K., Emissions Reductions in Diesel and Kerosene Flames Using a Novel Fuel Injector, *Journal of Propulsion and Power*. Vol. 25, No. 4, 2009.
- Sadasivuni, V., Agrawal, A. K., A novel meso-scale Combustion System for Operation with Liquid Fuels, *Proceedings of the Combustion Institute*, 32, pp. 3155–3162, 2009.
- Wünnig, J. A., Wünnig, J. G., Flameless Oxidation to Reduce Thermal No-formation, *Progress in Energy and Combustion Science*, 23, Issue 1, pp.81-94, 1997.